THE ASTROPHYSICAL JOURNAL, 560:L105–L109, 2001 October 10

EVOLUTION OF TWO EIT/Hα MORETON WAVES

A. WARMUTH,[1] B. VRŠNAK,[2] H. AURASS,[3] AND A. HANSLMEIER[1]
Received 2001 May 23; accepted 2001 August 28; published 2001 September 21

ABSTRACT

Since the discovery of EIT waves, questions have remained about the driver of these disturbances and their association with the chromospheric Moreton waves. In order to resolve some of these issues, two flare-associated transient events (1997 November 3 and 1998 May 2) observed simultaneously in Hα and EIT are analyzed. The cospatiality of Moreton and EIT wave fronts is established, and a deceleration of the disturbances is found in both events. In the case of 1998 May 2, a detailed analysis of the evolution of the Moreton wave, its kinematics, and perturbation profile is carried out. The results—deceleration, broadening, and decrease of intensity of the profiles—favor the fast-mode shock ("blast wave") scenario over the coronal mass ejection–associated magnetic field evolution hypothesis.

Subject headings: shock waves — Sun: chromosphere — Sun: corona — Sun: flares

1. INTRODUCTION

The recent discovery of the so-called EIT wave phenomenon (Thompson et al. 1998), a globally propagating coronal disturbance typically appearing as a bright rim observed with the EUV Imaging Telescope (EIT) aboard *SOHO*, has sparked a new interest in Hα Moreton waves (Moreton & Ramsey 1960), which for a long time have been suspected to represent the chromospheric signature of coronal shocks (Uchida 1968). In particular, a lively debate on the drivers of these coronal disturbances has developed.

In the "blast-wave" scenario (Steinolfson et al. 1978), a flare produces an initial pressure pulse that propagates through the corona as a fast-mode MHD shock (Vršnak & Lulić 2000). There, the shock is observed as the bright fronts seen in EIT and as metric type II bursts (Uchida 1974), whereas the Moreton waves seen in Hα represent the chromospheric ground tracks of the dome-shaped coronal shock front (Uchida, Altschuler, & Newkirk 1973). Conversely, the proponents of the "piston mechanism" argue that coronal mass ejections (CMEs) are responsible for the initiation of the shocks (see Cliver, Webb, & Howard 1999 and references therein). Delannée & Aulanier (1999) have recently proposed a completely different interpretation of the EIT waves, which they believe not to be a signature of a shock wave at all but rather the result of opening magnetic field lines associated with a CME.

However, up until now the data have not been sufficient to prove any of these models. In particular, the association between EUV EIT waves and Hα Moreton waves is still not completely resolved (therefore, we will use the term Moreton wave only in conjunction with Hα observations). Statistical surveys of Moreton (Smith & Harvey 1971) and EIT waves (Klassen et al. 2000) have shown that on the average the former propagate 2–3 times faster than the latter, yet it follows from the theory of Uchida (1968) that they should be relatively cospatial, and indeed Thompson et al. (2000) report such a case. Unfortunately, their data were insufficient to determine how closely the two phenomena overlap. Consequently, in addition to the question of the driving agent, doubts remain whether Hα and EIT waves are indeed manifestations of the same process. Since the EIT waves show a wide variety of morphological patterns, there might even be distinct classes that are caused by different physical processes.

We will investigate the exact temporal and spatial relation between the wave fronts seen in EUV and Hα in the 1B/M1.4 flare of 1997 November 3 (henceforth denoted as E1) and the 3B/X1.1 flare of 1998 May 2 (E2). Unfortunately, in E1 the Hα wave was only observed in a single image of moderate quality, while in E2 we have captured the whole evolution of a Moreton wave, providing a detailed analysis of the evolution of the perturbation and its kinematics.

2. OBSERVATIONS

EIT (Delaboudinière et al. 1995) full-disk images at 195 Å (Fe XII) were used for coronal observations. EIT has a temporal cadence of ≈10–30 minutes and a spatial resolution of $2\farcs6$ pixel^{-1}. Hα full-disk images were provided by the Kanzelhöhe Solar Observatory for E1 (35 mm film, temporal cadence of 4 minutes) and E2 (digital Hα camera, cadence ≈1 minute, spatial resolution of $2\farcs3$ pixel^{-1}; see Messerotti et al. 1999).

The relevant data for the two events we have studied are given in Table 1. Optical observations of E2 and active region evolution are discussed in Warmuth et al. (2000), while Pohjolainen et al. (2001) treat primarily radio observations. E2 was associated with a bright partial-halo CME, while it is difficult to determine the CME association for E1. It probably produced only some very faint and slow ejections. For both flares, metric type II bursts were observed with the Potsdam radio spectrograph. The onset times of the flare waves were fixed by inspecting radio data (using the time of the impulsive emission in the decimeter to meter range). The location of the source was determined taking into account the shape of the wave fronts and the evolution of the Hα flare. In both events, the disturbances seemed to emanate from the edge of the flare, which was located in the periphery of the active region.

Figure 1 shows large-scale images of the two events in Hα and EIT with the overplotted locations of the wave fronts, which were determined visually using difference images. Also included are the paths (parts of great circles on a sphere of 1 $R_\odot$, which also accounts for foreshortening effects) along which we measured the projected photospheric distances $r(t)$ of the fronts from the probable starting point. The two sub-

[1] Institute for Geophysics, Astrophysics and Meteorology, University of Graz, Universitätsplatz 5, A-8010 Graz, Austria; ajw@igam.uni-graz.at, arnold.hanslmeier@uni-graz.at.
[2] Hvar Observatory, Faculty of Geodesy, Kačićeva 26, HR-10000 Zagreb, Croatia; bvrsnak@geof.hr.
[3] Astrophysikalisches Institut Potsdam, An der Sternwarte 16, D-14482 Potsdam, Germany; haurass@aip.de.

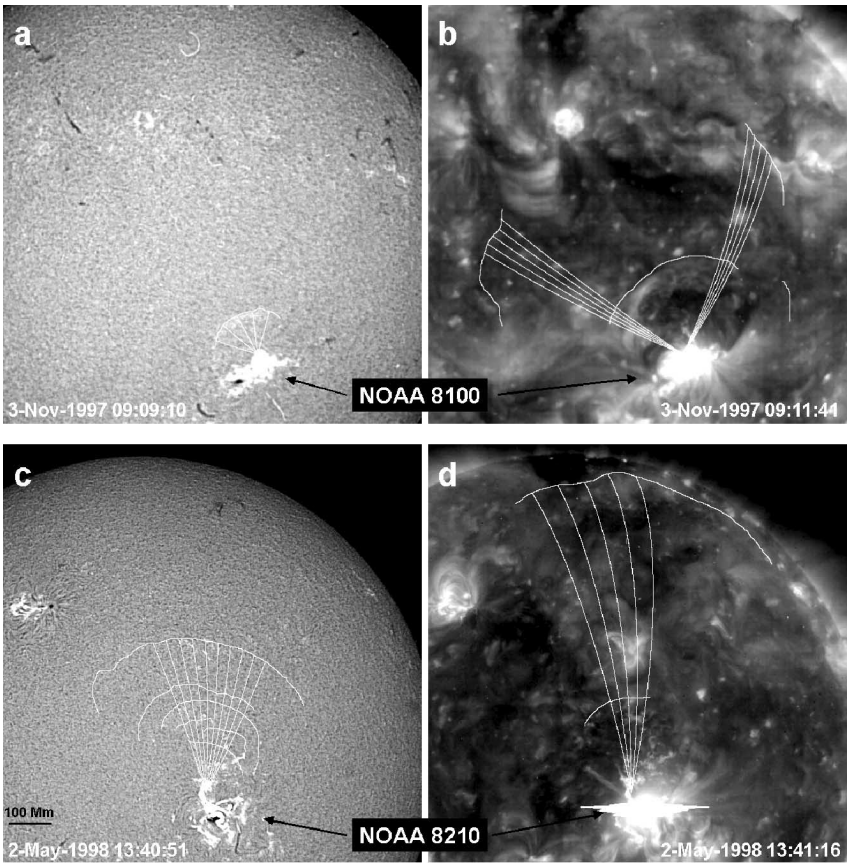

FIG. 1.—Hα (*left panels*) and EIT (*right panels*) images for E1 and E2. Overplotted are wave fronts and parts of great circles along which the distances $r(t)$ from the supposed origin of the disturbance were measured. Times (in UT) for the wave fronts are (*a*) 09:09:10; (*b*) 09:11:41, 09:33:41; (*c*) 13:38:57, 13:39:47, 13:40:51, 13:41:55, 13:44:57; and (*d*) 13:41:16, 14:11:15. West is to the right, and solar north is up.

images in Hα and EIT that are closest in time, enlarged in Figure 2, reveal the close association between the two signatures.

The measured values of $r(t)$ are shown in Figure 3 for both events. From E2, it is evident that the EIT and Hα disturbances are closely associated since they lie on the same kinematical curve. It should be noted that the $r(t)$ for the last EIT wave front is just a lower estimate since its leading edge could not be identified. Applying a second-degree polynomial least-squares fit to the measured $r(t)$ yields a deceleration of $\bar{a} = 150$ m s^{-2} (see Fig. 3). In E1, the data provide only an order of magnitude estimate of $\bar{a} = 100$ m s^{-2}. Let us note that in Thompson et al. (1999) the two measured westward-heading elements of the wave front also show a deceleration (see Fig. 4 therein).

In E1, the velocity changed from roughly 1000 km s^{-1} (utilizing the supposed starting time/location of the perturbation and the single Hα wave front as references) to some 250 km s^{-1} (derived from the two EIT wave fronts) in late stages. In E2, the positions of the earliest two Hα fronts reveal the velocities of different perturbation elements ranging between 650 and 1050 km s^{-1} with an average value of ≈900 km s^{-1}. At large distances, the velocity of the disturbance dropped down to about 400 km s^{-1}.

In E2, we were able to determine the intensity profile of the Hα perturbation and to follow its evolution. Profiles were obtained for a large number of directions (so that each pixel in the measured sector was sampled at least once) and then averaged laterally over the complete sector angle (see Fig. 1). From these profiles, we deduced the maximum intensity $I(t)$ and the locations of the leading edge $r_b(t)$, the intensity maximum $r_m(t)$, and the trailing edge $r_e(t)$, defining the perturbation width $w(t) = r_b - r_e$. The results show deceleration, profile broadening, and intensity decrease (Fig. 4).

3. DISCUSSION AND CONCLUSION

Usually, mean velocities are considered to characterize Moreton and EIT wave propagation; i.e., the speed of the perturbation is treated as constant. The presented analysis shows that this can be misleading, causing an artificial discrepancy between EIT and Hα signatures (see Klassen et al. 2000). For example, in E2 the mean Hα velocity (taking the mean speeds

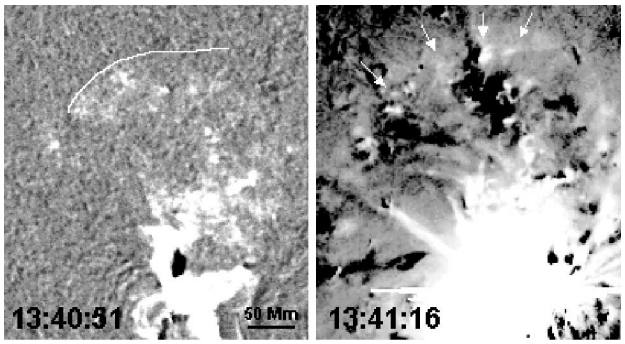

FIG. 2.—Enlarged difference subframes of E2: Hα (*left*) and EIT (*right*). Please note that EIT times are accurate to only ≈15 s. A preevent frame was subtracted from each image. The EIT wave front is indicated by the arrows. The location of its leading edge is plotted on the Hα image.

TABLE 1
THE TWO EIT/Hα MORETON WAVES AND THEIR ASSOCIATED FLARES AND CMES

Event	Class	Associated Flare Location	Start–Maximum (UT)	Disturbance Estimated Start (UT)	Hα Wave Start–End (UT)	EIT Wave Start–End (UT)	CME Speed (km s^{-1})
E1: 1997 Nov 3	1B/M1.4	S16°, W18°	09:03–09:10	09:07:30	09:09:10	09:11–09:33	?
E2: 1998 May 2	3B/X1.1	S15°, W14°	13:31–13:42	13:37:49	13:39–13:45	13:41–14:11	1039

averaged over all paths and wave fronts) is 700 km s^{-1}, whereas the mean EIT speed is only 400 km s^{-1}. If the decelerating motion is a general property of these disturbances, their EIT signatures *must* on average have lower mean velocities than their Hα counterparts since the former are usually traceable to much larger distances. The discrepancy is additionally increased due to the low cadence of the EIT observations, which provides only a poor coverage of fast events.

The close association between Hα and EIT waves (at least for these kinds of events; there might be EIT "waves" produced by a totally different mechanism that are not associated with Hα waves) is directly evident from the images shown in Figure 2. The disturbances are almost cospatial, but since the EIT times are accurate to only about 15 s, it is still not possible to determine which wave is the leading one. However, the images show that in the western part of the propagation region, where the disturbance seems to encounter an obstacle (a darkened patch in EIT), the Hα front has become slightly distorted and

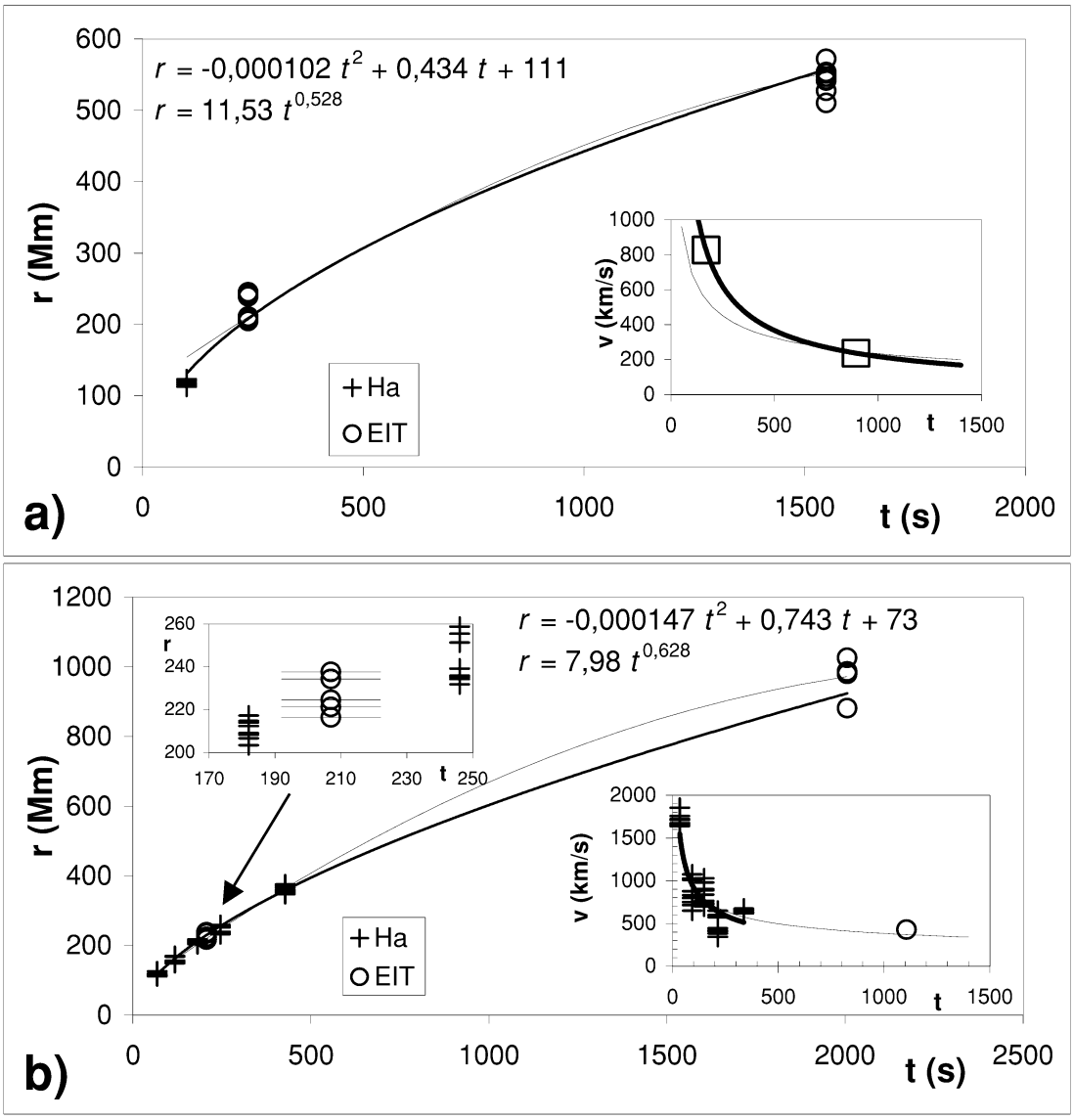

FIG. 3.—Propagation of the wave fronts of (*a*) E1 and (*b*) E2 (in the inset above the curves an enlarged part of the graph shows the close association of the Hα and EIT fronts; error bars are included for the EIT times). Power-law (*thick curve*) and second-degree polynomial (*thin curve*) fits are shown. In the inset in (*a*), the squares are velocities obtained using the mean r and t of Hα and EIT: $v = (r2 - r1)/(t2 - t1)$; $t = (t2 + t1)/2$. The thick line is a power-law fit, and the thin line is the derivative of $r(t)$ shown in the main graph. In the lower inset in (*b*), crosses are velocities using all Hα pairs, and the circle is the speed obtained using the two EIT fronts. The thick line is a fit through the Hα $v(t)$ points, and the thin line is as in (*a*).

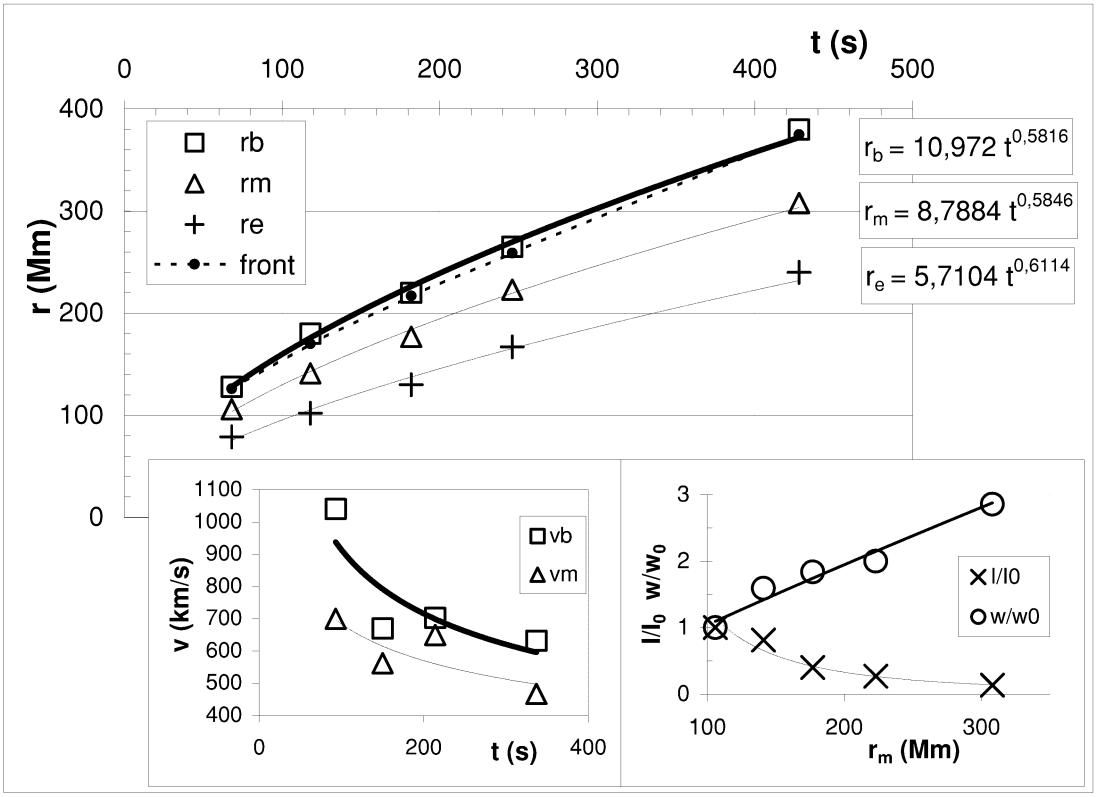

FIG. 4.—*Top:* Propagation of the Hα disturbance in E2 as inferred from its intensity profile. Note that the outermost parts of the visually determined wave fronts (*dashed line*; taken from Fig. 1) are located only slightly behind the leading edge of the profile. *Bottom left:* velocities obtained from neighboring fronts (as in Fig. 3). *Bottom right:* intensity and width of the profile normalized with respect to the value at $t = 68$ s.

slower as compared to EIT. In the previous two Hα frames, the Moreton front was traversing an elongated bright structure—which seemed to have been activated by the presence of the wave—and was split into two parts: the section that had traveled through the bright structure had become slower than the part that had been propagating through an apparently undisturbed medium. This happened on a timescale of ≈2 minutes and was therefore not seen in EIT.

The basic features of the observed disturbances are deceleration, broadening, and weakening. Such a behavior is characteristic for the shock waves that are formed from a large-amplitude simple wave (Landau & Lifshitz 1987). As the perturbation propagates, the profile broadens because the leading (shocked) edge moves faster than the trailing one. The frontal edge propagates at the velocity $v_f = Mv_{\rm MS}$ (where $v_{\rm MS}$ is the magnetosonic speed and M is the corresponding Mach number), whereas the trailing one propagates at $v_e = v_{\rm MS}$ (neglecting rarefaction). Let us note that the measured $r_e(t)$ reveals deceleration rather than constant velocity (Fig. 4), implying that the real trailing edge was not in fact resolved.

Both Mann et al. (1999; also discussed in Klassen et al. 2000) and Wang (2000) find fast-mode speeds of a few hundred kilometers per second in the low corona outside of active regions. The velocities at large distances (200–400 km s^{-1}; see insets in Fig. 3) are fairly consistent with these values. This implies that EIT waves can still be detected at low Mach numbers. In Hα, however, the disturbance is visible only in earlier stages when the Mach number is still relatively high, since it is more difficult to perturb the inert chromosphere. This can explain the higher rate of occurrence of EIT waves compared to Moreton events, since weak disturbances, which are probably initiated more frequently, will not show up in Hα. The mentioned "velocity discrepancy" is further increased by this effect.

The velocities measured at the time when the two studied Hα disturbances had faded away indicate that the Hα perturbance can be observed only if the Mach number is, say, $M > 2$. For comparison, taking $v_{\rm MS} \approx 300$ km s^{-1}, the Mach number at the beginning of the observable propagation can be estimated to roughly $M > 3$. Adopting the ratio of plasma to magnetic pressure as $\beta \approx 1$ (Mann et al. 1999) and $M = 3$, the density and the pressure jump across the shock (Benz 1993) can be estimated to 2.9 and 15, respectively.

In conclusion, the presented observations reveal the close association of the Hα and EIT disturbances. The deceleration caused by a decreasing shock amplitude can straightforwardly explain the discrepancy between the average Moreton and EIT wave speeds. This fast-mode shock wave scenario is favored over the magnetic field evolution hypothesis of Delannée & Aulanier (1999) since (1) the deceleration of the disturbance and its intensity profile evolution (broadening and intensity decrease) is consistent with the blast-wave scenario, (2) the wave fronts are centered on the flaring site (this was also found by Thompson et al. 2000) or, more precisely, on its edge, and (3) in E2, the Moreton wave front was deformed by two low-lying obstacles implying a propagation of information through a medium, which is characteristic of a wave.

Although we cannot completely rule out the CME-induced piston mechanism on the basis of these observations, we believe that the blast-wave scenario provides a more convincing explanation, especially since in contrast to E2, there was no clear CME association in E1, yet the wave fronts were just as fast and very pronounced. However, a blast-type shock could be

launched by ejecta of a smaller scale (e.g., sprays or ejecta observed with the *Yokhoh* soft X-ray telescope [SXT]; see, for example, Klein et al. 1999) instead of an initial pressure pulse. They could act as a temporary piston, and either they could generate a perturbation that then steepens into a shock or there could be a short phase of a driven shock, after which the shock propagates freely.

In the end, let us add that in E1 a propagating front was also imaged by the *Yohkoh* SXT (J. Khan 2001, private communication). The interpolated positions of the SXT wave agree well with the Hα and EIT fronts, which is another strong argument for a common exciting agent.

We thank B. J. Thompson for the provision of corrected EIT times. A. W. and A. H. acknowledge the support of the Austrian FWF project P13653-PHY.

REFERENCES

Benz, A. O. 1993, Plasma Astrophysics (Dordrecht: Kluwer)
Cliver, E. W., Webb, D. F., & Howard, R. A. 1999, Sol. Phys., 187, 89
Delaboudinière, J.-P., et al. 1995, Sol. Phys., 162, 291
Delannée, C., & Aulanier, G. 1999, Sol. Phys., 190, 107
Klassen, A., Aurass, H., Mann, G., & Thompson, B. J. 2000, A&AS, 141, 357
Klein, K.-L., Khan, J. I., Vilmer, N., Delouis, J.-M., & Aurass, H. 1999, A&A, 346, L53
Landau, L. D., & Lifshitz, E. M. 1987, Fluid Mechanics (2d ed.; Oxford: Pergamon)
Mann, G., et al. 1999, in Proc. Eighth *SOHO* Workshop: Plasma Dynamics and Diagnostics in the Solar Transition Region and Corona, ed. B. Kaldeich-Schürmann (ESA SP-446; Noordwijk: ESA), 477
Messerotti, M., et al. 1999, in Proc. ESA Workshop on Space Weather, ed. N. Crosby (WPP-155; Noordwijk: ESA), 321
Moreton, G. E., & Ramsey, H. E. 1960, PASP, 72, 357
Pohjolainen, S., et al. 2001, ApJ, 556, 421
Smith, S. F., & Harvey, K. L. 1971, in Physics of the Solar Corona, ed. C. J. Macris (Dordrecht: Reidel), 156
Steinolfson, R. S., Wu, S. T., Dryer, M., & Tandberg-Hanssen, E. 1978, ApJ, 225, 259
Thompson, B. J., Plunkett, S. P., Gurman, J. B., Newmark, J. S., St. Cyr, O. C., & Michels, D. J. 1998, Geophys. Res. Lett., 25, 2465
Thompson, B. J., et al. 1999, ApJ, 517, L151
———. 2000, Sol. Phys., 193, 161
Uchida, Y. 1968, Sol. Phys., 4, 30
———. 1974, Sol. Phys., 39, 431
Uchida, Y., Altschuler, M. D., & Newkirk, G., Jr. 1973, Sol. Phys., 28, 495
Vršnak, B., & Lulić, S. 2000, Sol. Phys., 196, 181
Wang, Y.-M. 2000, ApJ, 543, L89
Warmuth, A., et al. 2000, Sol. Phys., 194, 103